

Article

Generation and Nonlinear Dynamical Analyses of Fractional-Order Memristor-Based Lorenz Systems

Huiling Xi ^{1,2}, Yuxia Li ^{1,*} and Xia Huang ¹

¹ College of Electrical Engineering and Automation, Shandong University of Science and Technology, No. 579, Qianwan'gang Road, Qingdao Economic and Technical Development Zone, Qingdao 266510, China; E-Mails: cxhhl@126.com or xihuiling@nuc.edu.cn (H.X.); huangxia.qd@gmail.com (X.H.)

² Department of Mathematics, North University of China, No. 3, Xueyuan Road, Jiancaoping District, Taiyuan 030051, China

* Author to whom correspondence should be addressed; E-Mail: yuxiali2004@aliyun.com; Tel.: +86-13853200896; Fax: +86-532-86057153.

External Editor: Hai Yu and Guanrong Chen

Received: 1 October 2014; in revised form: 9 November 2014 / Accepted: 21 November 2014 /

Published: 28 November 2014

Abstract: In this paper, four fractional-order memristor-based Lorenz systems with the flux-controlled memristor characterized by a monotone-increasing piecewise linear function, a quadratic nonlinearity, a smooth continuous cubic nonlinearity and a quartic nonlinearity are presented, respectively. The nonlinear dynamics are analyzed by using numerical simulation methods, including phase portraits, bifurcation diagrams, the largest Lyapunov exponent and power spectrum diagrams. Some interesting phenomena, such as inverse period-doubling bifurcation and intermittent chaos, are found to exist in the proposed systems.

Keywords: fractional-order; memristor-based; Lorenz system

1. Introduction

The memristor, a nonlinear resistor with a memory effect, was originally postulated by Chua in 1971 [1]. Because there were no such devices found in reality, research on the memristor and its application did not attract attention in the science and engineering field. Its prototype was successfully

realized by researchers at Hewlett-Packard in 2008 [2]. Nowadays, the memristor has a wide range of applications in storage [3–5], neural networks [6–8], chaotic systems [9,10], and so on. It is observed that the memristor-based systems have properties that the common systems do not possess.

Recently, the memristor-based chaotic systems were becoming a research hotspot at home and abroad. In [10–13], Chua’s diodes were replaced with memristors characterized by a piecewise linear function. Bao *et al.* proposed an active two-terminal flux-controlled memristor characterized by a quadratic nonlinearity in [14]. In [15–18], flux-controlled memristors characterized by a smooth continuous cubic nonlinearity are presented. Furthermore, research has been done on the charge-controlled memristor characterized by a fourth degree polynomial function [19]. Compared to classical integer-order models, the fractional derivative provides a wonderful implement for describing the memory and hereditary properties of all kinds of materials and processes. Therefore, research on fractional-order systems has a more universal meaning. Recently, Ivo Petráš first studied the fractional-order memristor-based Chua’s circuit [20]. In [21], the simplest fractional-order memristor-based chaotic system is introduced. In [19], a fourth degree polynomial memristance function is used in the fractional-order memristor-based simplest chaotic circuit. The above-mentioned research results focus on the fractional-order memristor-based Chua or the simplest circuit. However, there are few results about the fractional-order memristor-based Lorenz system. In [22], an integer-order memristor-based Lorenz circuit with a piecewise linear memristance function is presented. Usually the equations of fractional-order systems are derived from the corresponding integer-order counterpart. Inspired by this, the idea of developing the fraction-order memristor-based Lorenz system with a piecewise linear function arose. In this paper, we first propose a new fractional-order memristor-based Lorenz system with the flux-controlled memristor characterized by a piecewise linear function, and its dynamical behaviors are illustrated by using a phase portrait, a bifurcation diagram, the largest lyapunov exponent and a power spectrum diagram. Then, what happens if the memristor is replaced with a quadratic nonlinearity, a cubic nonlinearity and a quartic nonlinearity, respectively? This paper gives the answer. Simulation results show that these fractional-order memristor-based systems exhibit some interesting dynamical behaviors within a certain range of parameters.

The organization of this paper is as follows. In Section 2, some preliminaries of fractional calculus and memristors are briefly reviewed. Section 3 presents the generation of fractional-order memristor-based Lorenz systems with four different flux-controlled memristors. In addition, the nonlinear dynamical behaviors of the proposed systems are analyzed. The conclusions are finally drawn in Section 4.

2. Preliminaries

2.1. Grünwald-Letnikov Fractional Derivative

Given that the method defined by Grünwald-Letnikov (GL) is the most direct numerical one to solve the fractional calculus in the various definitions of derivative [23–25], in this work, the q -th-order GL definition is given by [23,24]:

$${}_{\alpha_0}D_t^q f(t) = \lim_{h \rightarrow 0} h^{-q} \sum_{j=0}^{\frac{t-\alpha_0}{h}} (-1)^j \binom{q}{j} f(t - jh) \quad (1)$$

where:

$$\binom{q}{j} = \frac{q(q-1)\cdots(q-j+1)}{j!}.$$

Equation (1) can be reduced to:

$${}_{\alpha_0}D_t^q y(k) = h^{-q} \sum_{j=0}^k \omega_j^{(q)} y_{k-j}, \tag{2}$$

where:

$$\omega_j^{(q)} = (-1)^j \binom{q}{j}, j = 0, 1, 2, \dots$$

and h is the time step.

2.2. Memristor Model

At present, many memristor models have been proposed in [1,26,27]. The memristor model used in this paper is a flux-controlled memristor model described by the following circuit equations:

$$\begin{aligned} i &= W(\varphi)v, \\ \frac{d\varphi}{dt} &= v, W(\varphi) = \frac{dq(\varphi)}{d\varphi}, \end{aligned} \tag{3}$$

where i and v denote the current through and the voltage across the device; $q(\varphi)$ and $W(\varphi)$ are called the memristance and the memductance, respectively [17].

3. Fractional-Order Memristor-Based Lorenz Systems

In this section, four new fractional-order memristor-based Lorenz systems are introduced. In order to compare the nonlinear dynamical properties of these four systems under the same order, q is taken as 0.996 in the following sections.

3.1. Fractional-Order Lorenz System with the Flux-Controlled Memristor Characterized by a Piecewise Linear Function

An integer-order memristor-based Lorenz system with the piecewise linear function is described by [22]:

$$\begin{cases} \dot{x}_1(t) = -ax_1(t) - W(x_4(t))x_1(t) + bx_2(t), \\ \dot{x}_2(t) = cx_1(t) - x_2(t) - x_1(t)x_3(t), \\ \dot{x}_3(t) = x_1(t)x_2(t) - dx_3(t), \\ \dot{x}_4(t) = -x_1(t), \end{cases} \tag{4}$$

where $q_1(x_4(t))$ and $W(x_4(t))$ are given by:

$$q_1(x_4(t)) = \rho x_4(t) + 0.5(\sigma - \rho)(|x_4(t) + 1| - |x_4(t) - 1|), \tag{5}$$

$$W(x_4(t)) = \frac{dq_1(x_4(t))}{dx_4(t)} = \begin{cases} \sigma, & |x_4(t)| \leq 1, \\ \rho, & |x_4(t)| > 1. \end{cases} \tag{6}$$

The equations of the fractional-order memristor-based Lorenz system with the piecewise linear function are given by:

$$\begin{cases} D^q x_1(t) = -a_1 x_1(t) - W_1(x_4(t))x_1(t) + b_1 x_2(t), \\ D^q x_2(t) = c_1 x_1(t) - x_2(t) - x_1(t)x_3(t), \\ D^q x_3(t) = x_1(t)x_2(t) - d_1 x_3(t), \\ D^q x_4(t) = -x_1(t), \end{cases} \tag{7}$$

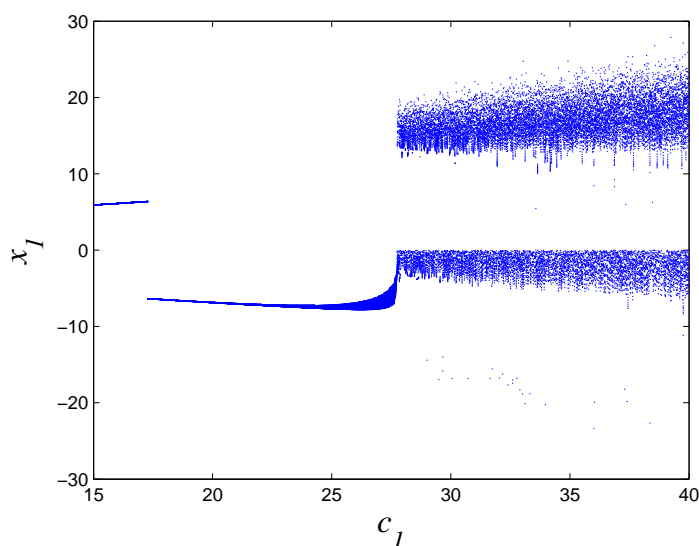
where q is the fractional-order satisfying $0 < q < 1$. $W_1(x_4(t))$ is the same as $W(x_4(t))$ in Equation (6).

The equations of System (7) are derived from the integer-order counterpart, but the value of system parameters of the original integer-order system cannot be applied to the fractional-order system directly. If the memristor is changed again to a quadratic nonlinearity, a cubic nonlinearity or a quartic nonlinearity memristance in the following sections, the choices of system parameters and the order q , which cause the systems to be of chaos, need a large amount of trial and error by numerical simulations and nonlinear dynamical analyses. In what follows, the nonlinear dynamical behaviors of System (7) are studied by a bifurcation diagram, the largest Lyapunov exponent, a phase portrait and a power spectrum diagram.

3.1.1. Bifurcation Analysis

Taking $a_1 = 8$, $b_1 = 15$, $d_1 = \frac{8}{3}$, $\sigma = 5$, $\rho = 8$ and $q = 0.996$, and changing the value of c_1 , the bifurcation diagram of System (7) when $c_1 \in [15, 40]$ is shown in Figure 1.

Figure 1. Bifurcation diagram of System (7) with respect to parameter c_1 .



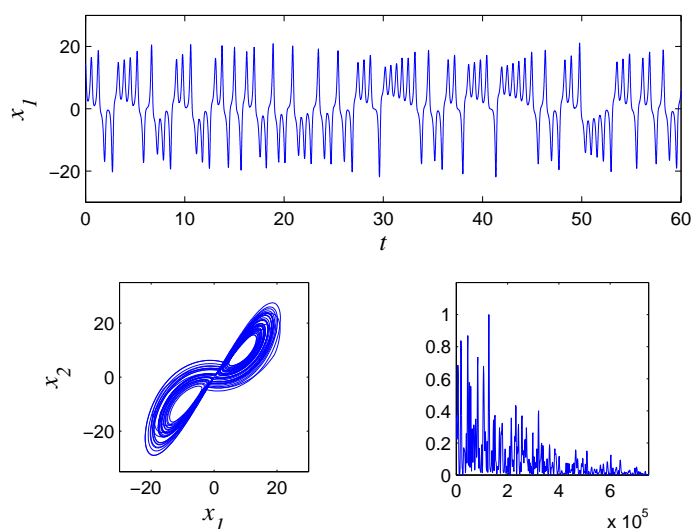
The change of the system parameter can lead to the sudden emergence, disappearance or mergence of the chaotic attractor in nonlinear dynamical systems, that is, the catastrophe. The catastrophe phenomena are ubiquitous in nonlinear systems. When the system parameters are altered to a critical state, the dynamical behavior of the system will suddenly change. In Figure 1, by means of numerical simulations, we can come to the conclusion that the system first jumps from a stable focus when $c_1 \in [15, 27.734]$

to a stable limit cycle when $c_1 = 27.735$, then from a stable limit cycle to an unstable focus when $c_1 \in [27.736, 27.742]$, then from an unstable focus to chaos when $c_1 \in [27.743, 40]$, with the increasing parameter c_1 .

3.1.2. The Largest Lyapunov Exponent, Phase Portrait and Power Spectrum Analysis

When $c_1 = 35$, using the method determining the value range of q by the largest Lyapunov exponent in [28,29], the new 4D fractional-order System (7) is chaotic for $0.988 \leq q < 1$. When $q = 0.996$, the largest Lyapunov exponent is 0.0022; the time history, phase portrait and power spectrum diagram of the chaotic attractor are shown as Figure 2.

Figure 2. Time history, phase portrait and power spectrum diagram of the chaotic attractor when $c_1 = 35$.



3.2. Fractional-Order Lorenz System with the Flux-Controlled Memristor Characterized by a Quadratic Nonlinearity

Based on the above-mentioned System (7), the piecewise linear function is replaced with a quadratic nonlinearity. Additionally, we can derive the equations of the fractional-order memristor-based Lorenz system with a quadratic nonlinearity from the integer-order counterpart [14]:

$$\begin{cases} D^q y_1(t) = -a_2 y_1(t) - W_2(y_4(t)) y_1(t) + b_2 y_2(t), \\ D^q y_2(t) = c_2 y_1(t) - y_2(t) - y_1(t) y_3(t), \\ D^q y_3(t) = y_1(t) y_2(t) - d_2 y_3(t), \\ D^q y_4(t) = -y_1(t), \end{cases} \tag{8}$$

where $q_2(y_4(t))$ and $W_2(y_4(t))$ are described by:

$$q_2(y_4(t)) = -\alpha_1 y_4(t) + 0.5 \beta_1 (y_4(t))^2 \operatorname{sgn}(y_4(t)), \tag{9}$$

$$W_2(y_4(t)) = \frac{dq_2(y_4(t))}{dy_4(t)} = -\alpha_1 + \beta_1 |y_4(t)|. \tag{10}$$

Similarly, we further investigate the nonlinear dynamical behaviors of System (8), including the bifurcation diagram, the largest Lyapunov exponent, phase portraits and power spectrum diagrams.

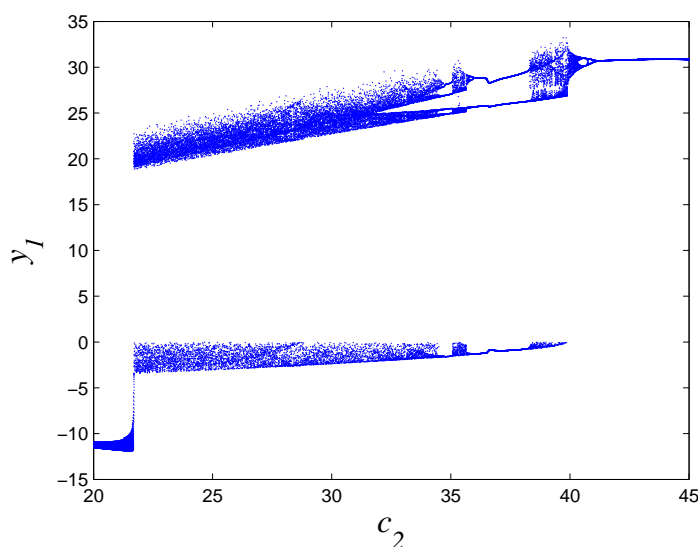
3.2.1. Bifurcation Analysis

Let $a_2 = 3.9$, $b_2 = 10$, $d_2 = \frac{8}{3}$, $\alpha_1 = -0.7 \times 10^{-3}$, $\beta_1 = 0.03 \times 10^{-3}$ and $q = 0.996$. Figure 3 shows the bifurcation diagram of System (8) when $c_2 \in [20, 45]$. The most interesting phenomenon is the existence of the inverse period-doubling bifurcation with the increasing of parameter c_2 .

From Figure 3, we can obtain the following dynamical behaviors:

- (1) System (8) undergoes the bifurcation from a stable focus to an unstable focus when $c_2 \in [20, 21.641]$;
- (2) The first inverse period-doubling bifurcation from chaos beginning at $c_2 = 21.642$ to the period-5 orbit when $c_2 \in [34.59, 35.06]$; the second inverse period-doubling bifurcation from chaos beginning at $c_2 = 35.07$ to the period-3 orbit when $c_2 \in [35.96, 38.3]$; the third inverse period-doubling bifurcation from chaos beginning at $c_2 = 38.31$ to the period-1 orbit when $c_2 \in [41.22, 45]$;
- (3) The occurrence of intermittent chaos.

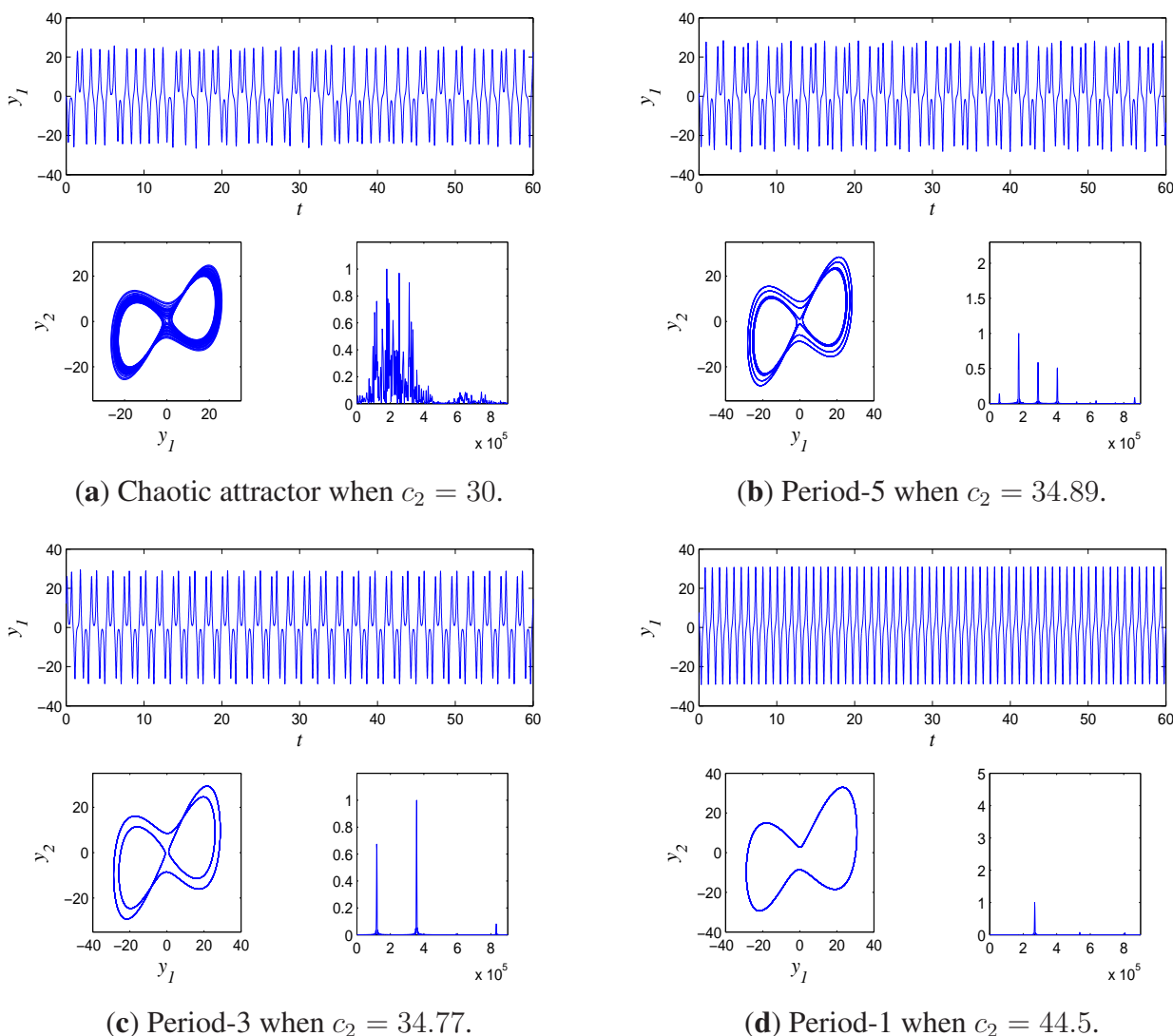
Figure 3. Bifurcation diagram of System (8) with respect to parameter c_2 .



3.2.2. The Largest Lyapunov Exponent, Phase Portraits and Power Spectrum Analysis

When $c_2 = 30$, we can determine that the new 4D fractional-order System (8) is chaotic for $0.992 \leq q < 1$ by the largest Lyapunov exponent. When $q = 0.996$, the largest Lyapunov exponent is 0.0239. Taking $c_2 = 30, 34.89, 34.77$ and 44.5 , respectively, and the time histories, phase portraits and power spectrum diagrams of chaotic attractor, the period-5 orbit, period-3 orbit and period-1 orbit are shown in Figure 4a–d, respectively.

Figure 4. Time histories, phase portraits and power spectrum diagrams of the chaotic attractor, period-5 orbit, period-3 orbit and period-1 orbit.



3.3. Fractional-Order Lorenz System with the Flux-Controlled Memristor Characterized by a Smooth Continuous Cubic Nonlinearity

Similarly, based on the above-mentioned System (7), the piecewise linear function is replaced with a cubic nonlinearity. Additionally, we can derive the equations of the fractional-order memristor-based Lorenz system with a cubic nonlinearity from the integer-order counterpart as [15–18]:

$$\begin{cases} D^q z_1(t) = -a_3 z_1(t) - W_3(z_4(t))z_1(t) + b_3 z_2(t), \\ D^q z_2(t) = c_3 z_1(t) - z_2(t) - z_1(t)z_3(t), \\ D^q z_3(t) = z_1(t)z_2(t) - d_3 z_3(t), \\ D^q z_4(t) = -z_1(t), \end{cases} \tag{11}$$

where $q_3(z_4(t))$ and $W_3(z_4(t))$ are described by:

$$q_3(z_4(t)) = \alpha_2 z_4(t) + \beta_2 (z_4(t))^3, \tag{12}$$

$$W_3(z_4(t)) = \frac{dq_3(z_4(t))}{dz_4(t)} = \alpha_2 + 3\beta_2(z_4(t))^2. \tag{13}$$

Moreover, the dynamical behaviors of System (11) are investigated by the same means.

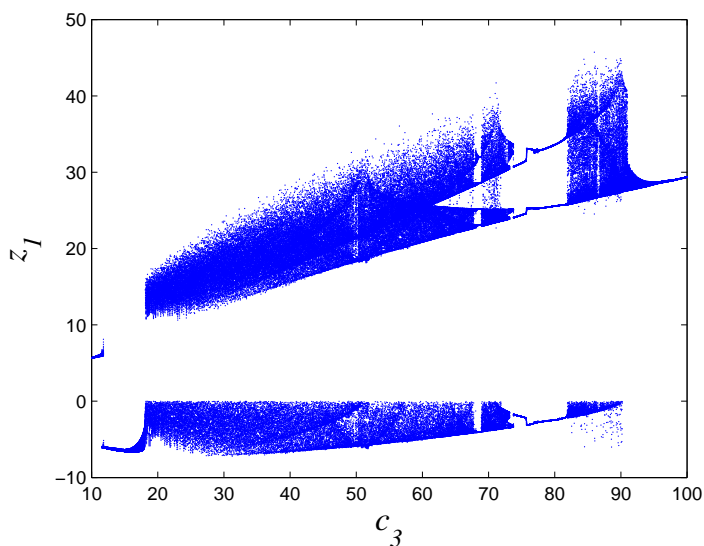
3.3.1. Bifurcation Analysis

Let $a_3 = 8$, $b_3 = 11$, $d_3 = \frac{8}{3}$, $\alpha_2 = 0.67 \times 10^{-3}$, $\beta_2 = 0.02 \times 10^{-3}$ and $q = 0.996$. The bifurcation diagram of System (11) when $c_3 \in [10, 100]$ is demonstrated in Figure 5. The phenomenon of the inverse period-doubling bifurcation exists in System (11), as well.

From Figure 5, the dynamical behaviors are analyzed as follows:

- (1) System (11) undergoes the bifurcation from a stable focus to an unstable focus when $c_3 \in [10, 18.12]$;
- (2) The first inverse period-doubling bifurcation from chaos beginning at $c_3 = 18.121$ to the period-5 orbit when $c_3 \in [67.84, 68.95]$; the second inverse period-doubling bifurcation from chaos beginning at $c_3 = 68.96$ to the period-3 orbit when $c_3 \in [73.77, 81.9]$; the third inverse period-doubling bifurcation from chaos beginning at $c_3 = 81.91$ to the period-1 orbit when $c_3 \in [97.83, 100]$;
- (3) The occurrence of intermittent chaos.

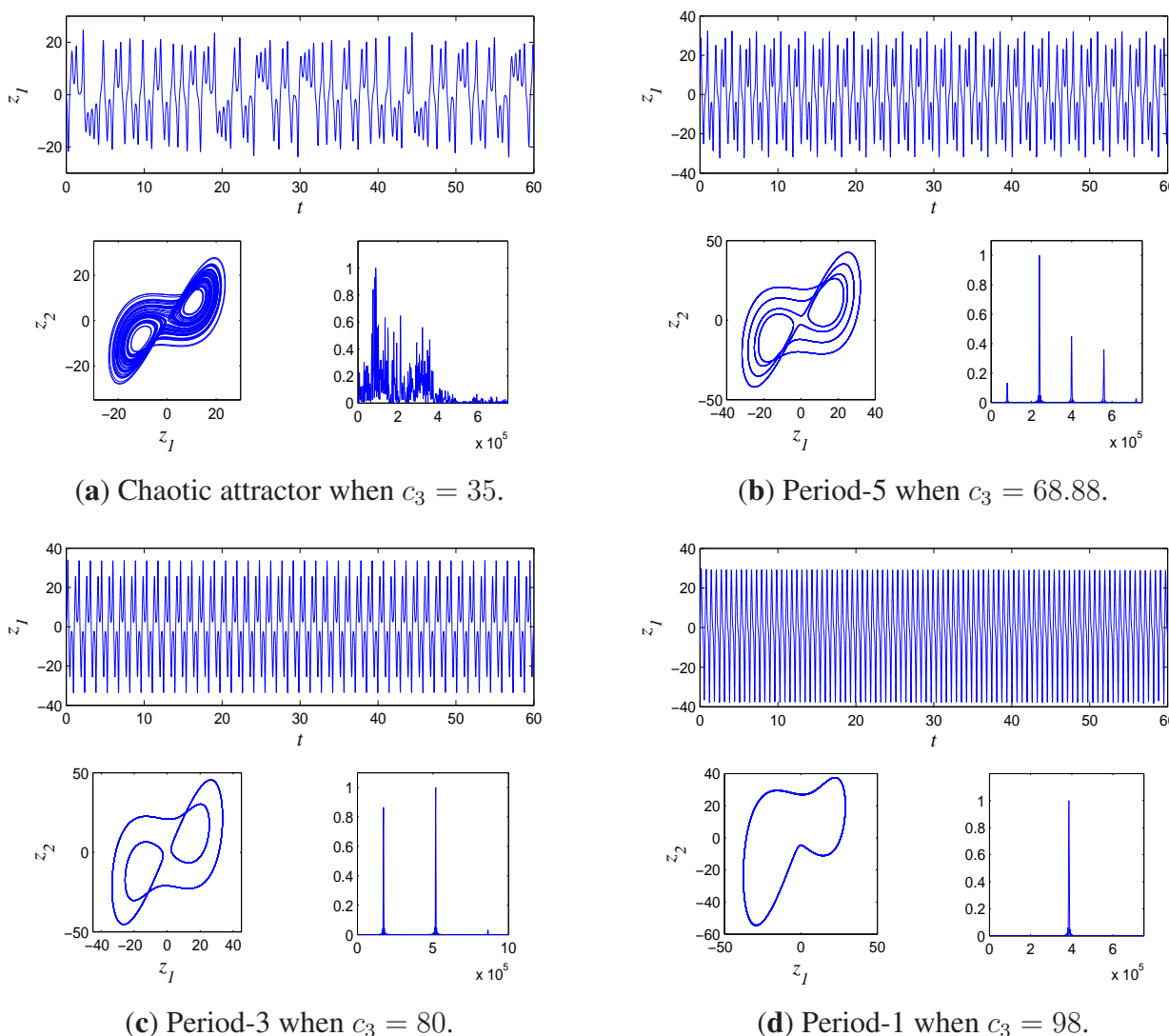
Figure 5. Bifurcation diagram of System (11) with respect to parameter c_3 .



3.3.2. The Largest Lyapunov Exponent, Phase Portraits and Power Spectrum Analysis

When $c_3 = 35$, the order of the new 4D fractional-order System (11) appearing as chaos is $0.984 \leq q < 1$ by the largest Lyapunov exponent. When $q = 0.996$, the largest Lyapunov exponent is 0.0234; taking $c_3 = 35, 68.88, 80$ and 98 , respectively. Figure 6a–d correspondingly shows time histories, phase portraits and power spectrum diagrams of chaotic attractor, period-5 orbit, period-3 orbit and period-1 orbit.

Figure 6. Time histories, phase portraits and power spectrum diagrams of the chaotic attractor, period-5 orbit, period-3 orbit and period-1 orbit.



3.4. Fractional-Order Lorenz System with the Flux-Controlled Memristor Characterized by a Quartic Nonlinearity

In this section, according to the charge-controlled memristor characterized by a fourth degree polynomial function in [19], the memristor in System (7) is replaced with the new flux-controlled memristor characterized by a quartic nonlinearity. Additionally, we can get the following equations of the fractional-order memristor-based Lorenz system with a quartic nonlinearity as:

$$\begin{cases} D^q w_1(t) = -a_3 w_1(t) - W_4(w_4(t))w_1(t) + b_3 w_2(t), \\ D^q w_2(t) = c_3 w_1(t) - w_2(t) - w_1(t)w_3(t), \\ D^q w_3(t) = w_1(t)w_2(t) - d_3 w_3(t), \\ D^q w_4(t) = -w_1(t), \end{cases} \tag{14}$$

where $q_4(w_4(t))$ and $W_4(w_4(t))$ are described by:

$$q_4(w_4(t)) = \alpha_3(w_4(t))^4 \text{sgn}(w_4(t)) + \beta_3(w_4(t))^2 \text{sgn}(w_4(t)) - \gamma_3, \tag{15}$$

$$W_4(w_4(t)) = \frac{dq_4(w_4(t))}{dw_4(t)} = 4\alpha_3|w_4(t)|^3 + 2\beta_3|w_4(t)|. \tag{16}$$

Furthermore, the dynamical behaviors of System (14) are studied by the same means.

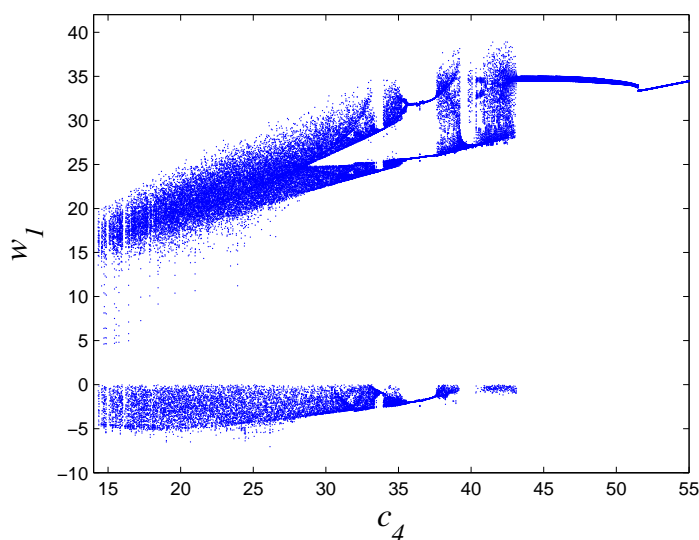
3.4.1. Bifurcation Analysis

Let $a_4 = 6.4$, $b_4 = 15.5$, $d_4 = 3.1$, $\alpha_3 = 0.63 \times 10^{-3}$, $\beta_3 = 0.025 \times 10^{-3}$ and $q = 0.996$. The bifurcation diagram of System (14) when $c_4 \in [14.32, 55]$ is shown in Figure 7.

By numerical simulations, the dynamical behaviors are analyzed as follows:

- (1) System (14) goes through the bifurcation from focus beginning at $c_4 = 14.32$ to chaos beginning at $c_4 = 18.41$;
- (2) The first inverse period-doubling bifurcation from chaos beginning at $c_4 = 18.41$ to the period-3 orbit when $c_4 \in [33.69, 34.09]$; the first quasi-period beginning at $c_4 = 34.1$ to the period-3 orbit when $c_4 \in [35.6, 37.69]$; the second inverse period-doubling bifurcation from chaos beginning at $c_4 = 37.7$ to the second quasi-period when $c_4 \in [42.175, 42.37]$ to the period-1 orbit when $c_4 \in [42.38, 55]$;
- (3) The occurrence of intermittent chaos.

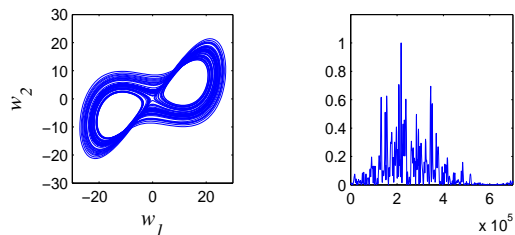
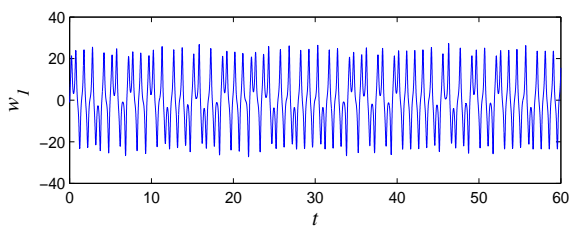
Figure 7. Bifurcation diagram of System (14) with respect to parameter c_4 .



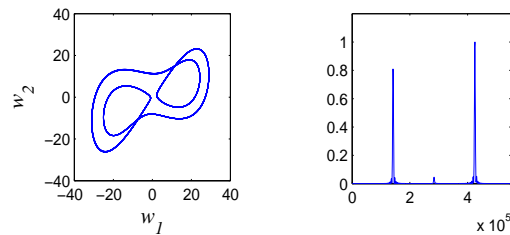
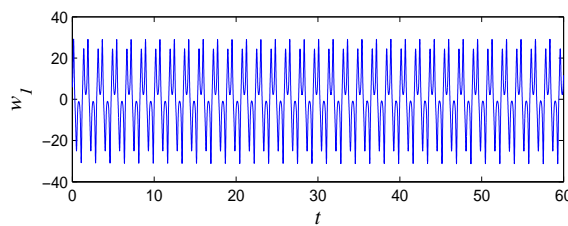
3.4.2. The Largest Lyapunov Exponent, Phase Portraits and Power Spectrum Analysis

When $c_4 = 26$, we can obtain that the new System (14) is chaotic for $0.984 \leq q < 1$ by the largest Lyapunov exponent. When $q = 0.996$, the largest Lyapunov exponent is 0.0174; taking $c_4 = 26, 33.92, 34.2, 37.27, 42.2$ and 54, respectively. Figure 8a–f correspondingly shows time histories, phase portraits and power spectrum diagrams of chaotic attractor, period-3 orbit, quasi-period orbit and period-1 orbit.

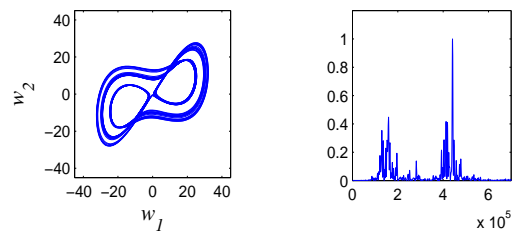
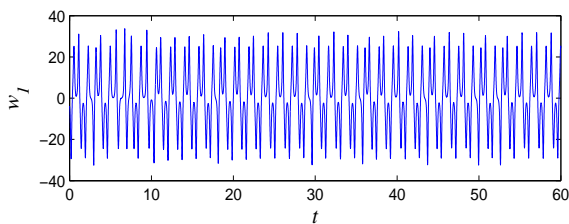
Figure 8. Time histories, phase portraits and power spectrum diagrams of the chaotic attractor, period-3 orbit, quasi-period orbit and period-1 orbit.



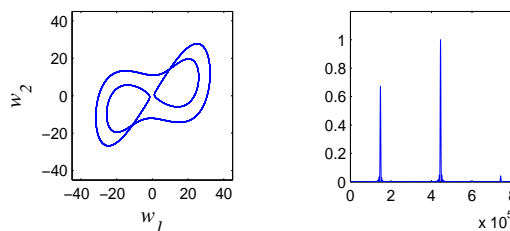
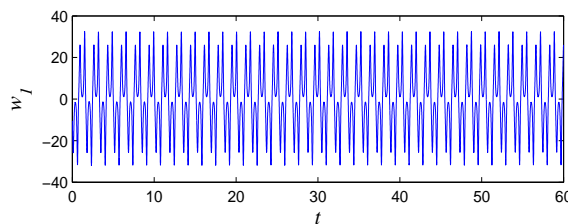
(a) Chaotic attractor when $c_4 = 26$.



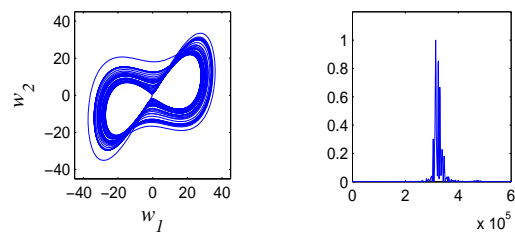
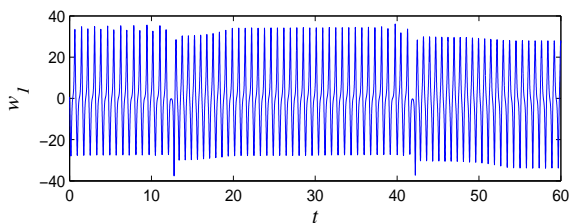
(b) Period-3 when $c_4 = 33.92$.



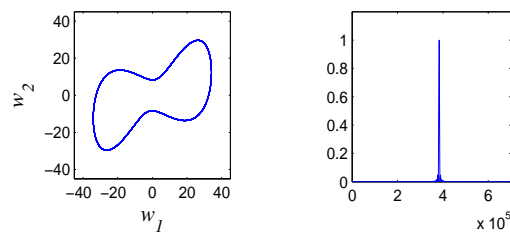
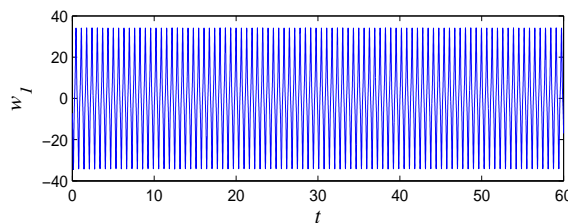
(c) Quasi-period when $c_4 = 34.2$.



(d) Period-3 when $c_4 = 37.27$.



(e) Quasi-period when $c_4 = 42.2$.



(f) Period-1 when $c_4 = 54$.

4. Conclusions

This paper introduced fractional-order memristor-based Lorenz systems with the flux-controlled memristor characterized by a piecewise linear function, a quadratic nonlinearity, a cubic nonlinearity and a quartic nonlinearity, respectively. Additionally, some interesting dynamical behaviors of these four systems are further demonstrated by computer simulations, including phase portraits, bifurcation diagrams, the largest Lyapunov exponent and power spectrum diagrams. Simulation results show that the introduction of a memristor leads to more complicated dynamical behaviors. We will provide a more detailed analysis in the next step. In addition, designing the new combination synchronization scheme for these four systems and constructing the fractional-order memristor-based Lorenz systems with a fifth or higher degree polynomial memristor will be our future work.

Acknowledgments

This work is supported by the National Natural Science Foundation of China under Grants 61473177 and 61473178. The authors also gratefully acknowledge the helpful comments and suggestions of the reviewers, which have improved the presentation.

Author Contributions

During the development of this project, we benefited from suggestions and critical insights provided by Yuxia Li and Xia Huang. Huiling Xi and Xia Huang gave the models and analysed all figures and data for the paper, and Huiling Xi wrote the paper. Correspondence and requests for materials should be addressed to Huiling Xi. All authors have read and approved the final manuscript.

Conflicts of Interest

The authors declare no conflicts of interest.

References

1. Chua, L.O. Memristor—the missing circuit element. *IEEE Trans. Circuit Theory* **1971**, *18*, 507–519.
2. Strukov, D.B.; Snider, G.S.; Stewart, D.R.; Williams, R.S. The missing memristor found. *Nature* **2008**, *453*, 80–83.
3. Sharifi, M.J.; Banadaki, Y.M. General spice models for memristor and application to circuit simulation of memristor-based synapses and memory cells. *J. Circuit Syst. Comput.* **2010**, *19*, 407–424.
4. Berzina, T.; Smerieri, A.; Bernabo, M.; Pucci, A.; Ruggeri, G.; Erokhin, V.; Fontana, M.P. Optimization of an organic memristor as an adaptive memory element. *J. Appl. Phys.* **2009**, *105*, doi:10.1063/1.3153944.
5. Eshraghian, K.; Cho, K.R.; Kavehei, O.; Kang, S.K.; Abbott, D.; Kang, S.M.S. Memristor MOS content addressable memory(MCAM): Hybrid architecture for future high performance search engines. *IEEE Trans. Very Large Scale Integr. Syst.* **2010**, *19*, 1407–1417.

6. Wen, S.; Zeng, Z.; Huang, T.; Chen, Y. Passivity analysis of memristor-based recurrent neural networks with time-varying delays. *J. Frankl. Inst.* **2013**, *350*, 2354–2370.
7. Wang, W.; Li, L.; Peng, H.; Xiao, J.; Yang, Y. Synchronization control of memristor-based recurrent neural networks with perturbations. *Neural Netw.* **2014**, *53*, 8–14.
8. Chen, J.; Zeng, Z.; Jiang, P. Global Mittag-Leffler stability and synchronization of memristor-based fractional-order neural networks. *Neural Netw.* **2014**, *51*, 1–8.
9. Barboza, R.; Chua, L.O. The four-element Chua's circuit. *Int. J. Bifurc. Chaos* **2008**, *18*, 943–955.
10. Itoh, M.; Chua, L.O. Memristor oscillators. *Int. J. Bifurc. Chaos* **2008**, *18*, 3183–3206.
11. Li, C.; Wei, M.; Yu, J. Chaos generator based on a PWL memristor. In Proceedings of the 2009 International Conference on Communications, Circuits and Systems, Milpitas, CA, USA, 23–25 July 2009; pp. 944–947.
12. Huang, J.; Li, C.; He, X. Stabilization of a memristor-based chaotic system by intermittent control and fuzzy processing. *Int. J. Control Autom. Syst.* **2013**, *11*, 643–647.
13. Zhong, Q.; Yu, Y.; Yu, J. Fuzzy modeling and impulsive control of a memristor-based chaotic system. *Chin. Phys. Lett.* **2010**, *27*, 020501.
14. Bao, B.; Xu, J.; Liu, Z. Initial state dependent dynamical behaviors in a memristor based chaotic circuit. *Chin. Phys. Lett.* **2010**, *27*, 070504.
15. Li, Y.; Huang, X.; Guo, M. The generation, analysis, and circuit implementation of a new memristor based chaotic system. *Math. Probl. Eng.* **2013**, *2013*, doi:10.1155/2013/398306.
16. Bao, B.; Liu, Z.; Xu, J. Steady periodic memristor oscillator with transient chaotic behaviours. *Electron. Lett.* **2010**, *46*, 228–230.
17. Bao, B.; Liu, Z.; Xu, J. Dynamical analysis of memristor chaotic oscillator. *Acta Phys. Sin.* **2010**, *59*, doi:10.7498/aps.59.3769.
18. Bao, B.; Hu, W.; Xu, J.; Liu, Z.; Zou, L. Analysis and implementation of memristor chaotic circuit. *Acta Phys. Sin.* **2011**, *60*, doi:10.7498/aps.60.120502.
19. Teng, L.; Iu, H.H.C.; Wang, X.Y.; Wang, X.K. Chaotic behavior in fractional-order memristor-based simplest chaotic circuit using fourth degree polynomial. *Nonlinear Dyn.* **2014**, *77*, 231–241.
20. Petráš, I. Fractional-order memristor-based Chua's circuit. *IEEE Trans. Circuits Syst. II* **2010**, *57*, 975–979.
21. Cafagna, D.; Grassi, G. On the simplest fractional-order memristor-based chaotic system. *Nonlinear Dyn.* **2012**, *70*, 1185–1197.
22. Wen, S.; Zeng, Z.; Huang, T.; Chen, Y. Fuzzy modeling and synchronization of different memristor-based chaotic circuits. *Phys. Lett. A* **2013**, *377*, 2016–2021.
23. Ho, M.; Hung, Y. Synchronization of two different systems by using generalized active control. *Phys. Lett. A* **2003**, *301*, 424–428.
24. Lin, J.; Yan, J.; Liao, T. Chaotic synchronization via adaptive sliding mode observers subject to input nonlinearity. *Chaos Solitons Fractals* **2005**, *24*, 371–381.
25. Zhao, L.; Shieh, L.S.; Chen, G.; Coleman, N.P. Simplex sliding mode control for nonlinear uncertain systems via chaos optimization. *Chaos Solitons Fractals* **2005**, *23*, 747–755.

26. Strukov, D.B.; Snider, G.S.; Stewart, G.R.; Williams, R.S. The missing memristor found. *Nature* **2008**, *453*, 80–83.
27. Chua, L.O.; Kang, S.M. Memristive devices and systems. *Proc. IEEE* **1976**, *64*, 209–223.
28. Zhou, P.; Huang, K. A new 4-D non-equilibrium fractional-order chaotic system and its circuit implementation. *Commun. Nonlinear Sci. Numer. Simul.* **2014**, *19*, 2005–2011.
29. Zhou, P.; Yang, F. Hyperchaos, chaos, and horseshoe in a 4D nonlinear system with an infinite number of equilibrium points. *Nonlinear Dyn.* **2014**, *76*, 473–480.

© 2014 by the authors; licensee MDPI, Basel, Switzerland. This article is an open access article distributed under the terms and conditions of the Creative Commons Attribution license (<http://creativecommons.org/licenses/by/4.0/>).